DMD Fast Forward. Published on February 2, 2018 as DOI: 10.1124/dmd.117.079061
This article has not been copyedited and formatted. The final version may differ from this version.

Title page

Inter-individual Differences in the Expression of ABC and SLC Family Transporters in Human Skin: DNA Methylation Regulates Transcriptional Activity of the Human *ABCC3* (MRP3) Gene

Tomoki Takechi, Takeshi Hirota, Tatsuya Sakai, Natsumi Maeda, Daisuke Kobayashi, and Ichiro Ieiri

Department of Clinical Pharmacokinetics, Graduate School of Pharmaceutical Sciences, Kyushu University, Fukuoka, Japan (T.T., T.H., T.S., N.M., I.I.); Drug Development Research Laboratories, Kyoto R&D Center, Maruho Co., Ltd., Kyoto, Japan (T.T.); and Department of Clinical Pharmacy and Pharmaceutical Care, Graduate School of Pharmaceutical Sciences, Kyushu University, Fukuoka, Japan (D.K.)

DMD Fast Forward. Published on February 2, 2018 as DOI: 10.1124/dmd.117.079061
This article has not been copyedited and formatted. The final version may differ from this version.

Running title page

Running title: DNA methylation regulates MRP3 expression in human skin

Corresponding author: Ichiro Ieiri

Department of Clinical Pharmacokinetics, Graduate School of Pharmaceutical Sciences, Kyushu University, 3-1-1 Maidashi, Higashi-ku, Fukuoka 812-8582, Japan.

Tel. +81-(0)92-642-6656, Fax. +81-(0)92-642-6660, E-mail: ieiri-ttr@umin.ac.jp

The number of text pages : 54

The number of tables : 4

The number of figures : 5

The number of references : 61

The number words in the Abstract : 240

The number words in the Introduction : 694

The number words in the Discussion : 1563

Abbreviations:

ABC, ATP-binding cassette; 5-aza-dC, 5-aza-2'-deoxycytidine; bp, base pairs; CGI, CpG island; COBRA, combined bisulfate restriction analysis; CRISPR, Clustered

regularly interspaced short palindromic repeats; GAPDH, glyceraldehyde 3-phosphate dehydrogenase; kbp, kilobase pair; MRP, multidrug resistance-associated protein; NHEK, normal human epidermal keratinocytes; SLC, solute carrier; SNP, single nucleotide polymorphism; TIS, translation start site

DMD Fast Forward. Published on February 2, 2018 as DOI: 10.1124/dmd.117.079061
This article has not been copyedited and formatted. The final version may differ from this version.

Abstract

The identification of drug transporters expressed in human skin and inter-individual differences in gene expression are important for understanding the role of drug transporters in human skin. In the present study, we evaluated the expression of ABC and SLC transporters using human skin tissues. In skin samples, ABCC3 was expressed at the highest levels, followed by SLCO3A1, SLC22A3, SLC16A7, ABCA2, ABCC1, and SLCO2B1. Among the quantitated transporters, ABCC3 accounted for 20.0% of the total mean transporter mRNA content. The expression of ABCC3 mRNA showed large inter-individual variability (9.5-fold). None of the SNPs tested (–1767G>A, –1328G>A, –1213C>G, –897delC, –260T>A, and –211C>T) in the promoter region of the *ABCC3* gene showed a significant change in ABCC3 mRNA levels. ABCC3 expression levels negatively correlated with the methylation status of the CpG island (CGI) located approximately 10 kbp upstream of *ABCC3* (*Rs*: –0.323, $P < 0.05$). The reporter gene assay revealed a significant increase in transcriptional activity in the presence of CGI. ABCC3 mRNA was up-regulated in HaCaT cells by the demethylating agent 5-aza-2'-deoxycytidine. Furthermore, the deletion of the region surrounding CGI using the CRISPR/Cas9 system resulted in significantly lower ABCC3 mRNA levels than those in control clones in HaCaT cells. We herein demonstrated that large inter-individual

differences in the expression of drug transporters in human skin. CGI may function as an enhancer of the transcription of *ABCC3* and methylation levels in CGI contribute to the variability of *ABCC3* expression in human skin.

Introduction

Membrane transporters have broad specificity and facilitate the uptake and efflux of their substrates across plasma membranes. Two major superfamilies, the ABC and SLC families, strongly influence the absorption, distribution, and excretion of drugs. Previous studies suggested that transporters play a role in *in vivo* drug pharmacokinetics, while transporter-mediated drug-drug interactions were recently identified (Schneck et al., 2004; Shitara et al., 2004; Neuvonen et al., 2006; Klatt et al., 2011). The accumulation of evidence has revealed that variabilities in the expression and activities of some transporters affect pharmacokinetics as well as pharmacological and/or toxicological effects (Cascorbi 2006; Maeda and Sugiyama, 2008; Ieiri et al., 2006; Gotanda et al., 2015).

Genetic polymorphisms are one of the most important factors influencing variable gene expression. Single nucleotide polymorphisms (SNPs) in pharmacokinetic-related genes play a critical role in inter-individual variations in pharmacokinetics and drug responses (Ieiri et al., 2009; Ma and Lu, 2011). In addition to genetic polymorphisms, epigenetic mechanisms, including DNA methylation in clusters of CpG dinucleotides, called CpG islands (CGI), also contribute to the variability of gene expression (Yasar et al., 2013). Previous studies indicated that DNA methylation plays an important role in the inter-

individual variability in drug transporter gene expression (Saito et al., 2011; Wu et al., 2015).

Skin is the largest organ in the human body. It consists of multiple layers: the stratum corneum, epidermis, dermis, and subcutaneous tissue, and acts as both a physical and chemical permeability barrier. The stratum corneum, the most superficial layer of the epidermis, is considered to be the major diffusion barrier that limits the transdermal penetration of xenobiotics. Notwithstanding this barrier function, a growing number of strategies (Lane, 2013; Ita, 2016) have been developed in order to deliver drugs to and through skin because transdermal delivery has a number of advantages, such as avoidance of the first-pass effect of the liver and the minimization of pain, over the oral, hypodermic, and intravenous routes (Prausnitz and Langer, 2008). Although the skin penetration of xenobiotics was previously attributed to passive diffusion, increasing evidence indicates that transporters have a function in the biochemical barrier of skin epithelial cells beneath the stratum corneum. For example, the constitutive expression of multidrug resistance proteins (MRPs) has been detected in normal human keratinocytes (NHEK), which is the predominant cell in the epidermis (Baron et al., 2001). Furthermore, previous studies showed that NHEK exhibit the functional transporter-mediated uptake and efflux activity (Schiffer et al., 2003; Heise et al., 2010). A recent transport study demonstrated that ABC

transporters in different compartments of the skin contribute to the transdermal absorption of a typical substrate in mice (Hashimoto et al., 2013). These findings suggest that transporters play an important role in the disposition of drugs, at least in murine skin and human keratinocyte cell cultures. However, it is important to note that previous studies using cell cultures, animal models, or only a small number of skin tissues were mostly inadequate for quantitative analyses of transporter expression in human skin. Large inter-individual variabilities in the expression of transporters may lead to inappropriate drug concentrations, causing drug toxicity or insufficient therapeutic effects in skin. Therefore, inter-individual variability in the expression levels of transporters need to be identified by evaluating expression levels in a large number of skin tissues.

The aims of the present study were to assess the expression levels of ABC and SLC transporters in human skin and elucidate the mechanisms responsible for variability in mRNA expression. The transporters analyzed (26 ABC and 25 SLC transporters) were selected based on their relevance as drug transporters (FDA, 2012; EMA, 2012; International Transporter Consortium, 2010; Roth et al., 2012) and previous studies showing transporter expression in human skin (Baron et al., 2001; Schiffer et al., 2003; Kielar et al., 2003; Markó et al., 2012). We examined genetic variations in the promoter regions of *ABCC3*, which showed large inter-individual variability in expression levels in

this study. We performed a DNA methylation analysis to clarify the relationship between the methylation status and mRNA levels in human skin. The contribution of CGI to ABCC3 expression was examined using the luciferase reporter assay and a deletion analysis of CGI in HaCaT cells using the CRISPR/Cas9 system.

Materials and Methods

Skin Tissues

Human full-thickness skin tissues from 48 Caucasian females were purchased from BIOPREDIC International (France). The skin tissues were derived from healthy adults. The average (± SD) age of the skin tissue donors was 45.9 ± 10.8 years, with a range of 22 to 64 years. Anatomical sites were abdomen (n=33) and breast (n=15). The donor information is summarized in Supplemental Table 1. All tissue specimens were obtained with informed consent, and this study was approved by the Ethics Committee at Kyushu University.

Cell Culture

A HaCaT human keratinocyte line was obtained from Cell Lines Service (Heidelberg, Germany). HaCaT cells were grown in Dulbecco's modified Eagle's medium (Sigma Aldrich, St. Louis, MO) supplemented with 10% fetal bovine serum (Nichirei Biosciences Inc., Tokyo, Japan) and incubated at 37°C in a 5% CO_2 atmosphere. The culture medium was replaced every 2 or 3 days. Cells were routinely passaged before reaching confluence.

Isolation of Total RNA from Human Skin and cDNA Synthesis

Total RNA was isolated from each tissue using an RNeasy Fibrous Tissue Mini Kit (Qiagen, Hilden, Germany). RNA samples were reverse-transcribed into first-strand cDNA with approximately 300 to 2000 ng total RNA, 1 × first strand buffer, 20 mM DTT, 0.5 μg random primer (Promega, Madison, Wisconsin), 2 mM dNTP mixture, and 200 units of SuperScript II RNase H- reverse transcriptase (Life Technologies, Carlsbad, CA). The reaction was run at 42°C for 60 min. Reverse transcription reactions were always performed in the presence or absence of reverse transcriptase in order to ensure that genomic DNA did not contaminate subsequent PCR. cDNA was stored at –30°C until used.

Quantitative Real-Time PCR

mRNA levels were measured by real-time PCR using an ABI PRISM 7000 sequence detection system (Applied Biosystems, Foster City, CA). The sequences of the primers used in this study are summarized in Supplemental Table 2. Amplification mixtures contained 5 μL of SYBR Premix Ex Taq (Takara, Kyoto, Japan), 0.2 μL of Rox reference dye, 2 μL of a cDNA synthesis mixture, 2 pmol each of the forward and reverse primers, and distilled water in a total volume of 10 μL. Cycling conditions were as follows: 30 seconds at 95°C, followed by 40 cycles of amplification at 95°C for 5 seconds and at

DMD Fast Forward. Published on February 2, 2018 as DOI: 10.1124/dmd.117.079061
This article has not been copyedited and formatted. The final version may differ from this version.

60°C for 30 seconds. The specificity of the real-time PCR product was proven by a dissociation curve analysis. Triplicate measurements were performed for all samples. In order to compare gene expression levels among different samples, the amount of target mRNA was corrected relative to that of GAPDH. GAPDH has been used as an internal reference in gene expression analysis using human skin (Takenaka et al., 2013; Fujiwara et al., 2014) and the expression of GAPDH showed a small inter-individual variation in human skin (Osman-Ponchet et al., 2014). Real-time PCR data for each target gene quantity were calculated in the following two ways.

The Pfaffl method: the target gene to GAPDH gene ratio was evaluated as follows:

$$\text{ratio} = E_{\text{target}}^{\Delta Ct\ \text{target (reference – test)}} / E_{\text{GAPDH}}^{\Delta Ct\ \text{GAPDH (reference – test)}}$$

where:

E_{target} : amplification efficiency of the target gene

E_{GAPDH} : amplification efficiency of the GAPDH gene

$\Delta C_{t\ \text{target}}$: the difference between C_t of the target gene in the reference sample and test sample

$\Delta C_{t\text{GAPDH}}$: the difference between C_t of the GAPDH gene in the reference sample and test sample

Absolute quantification: Each 96-well assay plate contained unknown samples and

sequentially diluted concentrations of the plasmid standard constructed, from which a standard curve was generated for the quantification of gene copy numbers in unknown samples.

Genotyping and Haplotype Analysis

Genomic DNA was isolated from skin specimens with a NucleoSpin Tissue kit (Macherey-Nagel GmbH & Co. KG, Germany) according to the manufacturer's protocol. Six SNPs (–1767G>A, –1328G>A, –1213C>G, –897delC, –260T>A, and –211C>T) in the promoter region of *ABCC3* (Sasaki et al., 2011; Lang et al., 2004) were genotyped in 48 skin donors by a PCR-restriction fragment length polymorphism analysis and direct sequencing. The sequences of primers are given in Supplemental Table 3. PCR was performed using approximately 10 ng of genomic DNA with 250 nM of each primer and AmpliTaq Gold DNA polymerase (Life Technologies) in a total volume of 10 μL. The following amplification conditions were used: an initial denaturation step of 95°C for 9 min followed by 40 cycles of denaturation at 95°C for 40 sec, annealing at 55.7 or 62.3°C for 45 sec, extension at 72°C for 40 sec, and a final extension at 72°C for 5 min. Regarding –1767G>A, PCR products were digested by *Bsm*A I and then electrophoresed on a 3% agarose gel. Direct sequencing using an ABI 3100 automatic sequencer (Applied

Biosystems) with a Big-Dye Terminator Cycle Sequencing Ready Reaction Kit (Applied Biosystems) was applied to all other SNPs. The sequence was inspected for deviations from the original *ABCC3* (GenBank accession No. NC_000017.11), which was defined as the reference. Haplotypes of the promoter region were estimated with ARLEQUIN Ver. 3.5 software. A linkage disequilibrium analysis was performed with Haploview (Broad Institute, Cambridge, MA, USA).

Bisulfite Conversion and Combined Bisulfate Restriction Analysis

CGIs located within 20 kbp up- and downstream of *ABCC3* were identified by the CpG Island Searcher Program (Takai and Jones, 2003). CGIs were defined using the following criteria: GC > 50%, observed CpG/expected CpG > 0.60, length > 200 bp, and the gap between an adjacent island > 100 bp. Bisulfite conversion and subsequent purification were performed using the EpiTect Bisulfite Kit (Qiagen) according to the manufacturer's protocol. Bisulfite-converted genomic DNA was subjected to PCR using bisulfite conversion-specific primers. PCR was performed by initial denaturation at 95°C for 9 min, followed by 40 to 45 cycles of 95°C for 40 sec, 50 to 65°C for 45 sec, 72°C for 40 sec, and finally by extension at 72°C for 5 min. PCR products were digested with each restriction enzyme based on a methylation-dependent restriction site. Primers for the

COBRA analysis and restriction enzymes are provided in Supplemental Table 4. The digested PCR products were electrophoresed on 3% agarose gels and visualized by ethidium bromide staining. The intensity of bands was quantified with LAS-3000 (Fujifilm, Tokyo, Japan). The proportion of methylated versus unmethylated DNA was assessed from the relative intensity of cut and uncut PCR products. Episcope-methylated HCT116 gDNA and unmethylated HCT116 DKO gDNA (TaKaRa) were used as the positive methylation and unmethylation controls, respectively.

Reporter Gene Vector Constructs

In the functional analysis of *ABCC3* CGI-6, three reporter gene vectors were constructed: pGL4.10-CGI, including CGI-6 ranging from –9954 to –9635 bp relative to TIS, pGL4.10-Pro, including the promoter ranging from –2013 to –1 bp relative to TIS, and pGL4.10-CGI/Pro, including CGI-6 and the promoter. The oligonucleotide sequences used for PCR are listed in Supplemental Table 5. The insert sequences of all resulting constructs were verified by direct sequencing.

Cell Transfection and Reporter Gene Assays

DMD Fast Forward. Published on February 2, 2018 as DOI: 10.1124/dmd.117.079061
This article has not been copyedited and formatted. The final version may differ from this version.

In reporter gene assays, 48.2 fmol of each vector construct with 25 ng of pRL-TK (Promega) as an internal control were transfected into HaCaT cells using Lipofectamine 3000 reagent (Life Technologies). Cells were harvested 48 hours after transfection, and firefly and renilla luciferase were both assayed using the Dual luciferase™ system reporter assay (Promega). Relative reporter gene activities were calculated by dividing the firefly luciferase activity of the reporter construct by the renilla luciferase activity of pRL-TK. Transfection was performed in triplicate and at least three independent experiments were conducted.

Demethylation Experiments in HaCaT Cells

HaCaT cells were treated with 3 μM 5-aza-2'-deoxycytidine (5-aza-dC; Sigma Aldrich) and 0.1% DMSO as a vehicle control for 72 hours. Total RNA was isolated from cells and ABCC3 mRNA expression levels were measured using quantitative real-time PCR.

Deletion of CGI using the CRISPR/Cas9 System

The pGL3-U6-sgRNA-PGK-puromycin vector (ID: 51133, Addgene, Cambridge, MA) and Guide-it™ CRISPR/Cas9 System Kit (TaKaRa) were used to generate vectors encoding a single guide RNA (sgRNA) and puromycin resistance or sgRNA and Cas9,

respectively. GuideRNAs targeting the CGI locus were designed using CRISPRdirect (http://crispr.dbcls.jp/). DNA oligonucleotides harboring 20 variable nucleotide sequences for Cas9 targeting were annealed to generate short double-strand DNA fragments with 4-bp overhangs compatible with ligation into the *Bsa*I site of the pGL3-U6-sgRNA-PGK-puromycin vector or pGuide-it CRISPR/Cas9 vector. In order to create a HaCaT cell line that deletes CGI-6, HaCaT cells were seeded on a 6-well plate at a density of 4.0×10^5 cells/well, and transfected using Lipofectamine 3000 (Life Technologies) with 2.5 μg of each vector. In order to select transfected cells, 1 μg/mL puromycin was added to the cell growth medium for 2 days. Cells were cloned by limiting dilutions, and DNA was extracted from the cloned cells for PCR amplification. PCR products were characterized by electrophoresis and sequencing in order to analyze the region deleted by the CRISPR/Cas9 system. ABCC3 mRNA expression in three deleted clones and four control clones was evaluated using a quantitative real-time PCR. The sequences of oligos and primers are described in Supplemental Table 6.

Statistical Analysis

Statistical analyses were conducted with R (version 3.0.0) and S plus. The Mann-Whitney U-test or Kruskal-Wallis rank sum test was applied to gene expression data stratified

according to genotype. Spearman's rank-order correlation analysis was used to test for correlations between the DNA methylation status and gene expression. In other cases, differences between groups were analyzed using the Student's *t*-test when only two groups were present. Differences were considered to be significant when *P* values were less than 0.05.

DMD Fast Forward. Published on February 2, 2018 as DOI: 10.1124/dmd.117.079061
This article has not been copyedited and formatted. The final version may differ from this version.

Results

Gene Expression of ABC and SLC Transporters in Human Skin

Sixteen out of the 51 transporter genes were present at the levels quantitated ($C_t < 31$), 21 were at the levels detected ($31 \leq C_t \leq 35$), and 14 were below the detection limit ($35 < C_t$, Table 1). Based on the results of the first screening, we selected transporters with a mean C_t value < 31 for absolute quantification. ABCB1 and ABCG2 transporters, which are transporters that are expressed in human skin, were added to the analysis. Quantification revealed that the expression of the *ABCC3* gene coding for the MRP3 transporter was the most abundant, followed by SLCO3A1, SLC22A3, SLC16A7, ABCA2, ABCC1, and SLCO2B1 (Figure 1A). Among the quantitated transporters, ABCC3 accounted for 20.0% of the total mean transporter mRNA content, while the top 3 transporters accounted for approximately half of the expression levels in human skin (Figure 1B). These results also indicated that the expression of ABCB1, ABCA7, and ABCG2 was very weak. Among the top 3 transporters in the quantification, inter-individual variations (n=48) in mRNA levels in ABCC3 and SLC22A3 were markedly greater (9.5- and 14.2-fold differences, respectively) than that in SLCO3A1 (4.2-fold). Typical substrates of the top 3 transporters are summarized in Supplemental Table 7.

DMD Fast Forward. Published on February 2, 2018 as DOI: 10.1124/dmd.117.079061
This article has not been copyedited and formatted. The final version may differ from this version.

ABCC3 Genetic Variants, Allele Frequencies, and Haplotypes

Six SNPs in the promoter region of *ABCC3* were genotyped in 48 skin samples of Caucasian female origin. Allele frequencies were 9.4, 2.1, 7.3, 32.3, 7.3, and 60.4% for –1767G>A (rs1989983), –1328G>A (rs72837520), –1213C>G (rs62059725), –897delC (rs35467079), –260T>A (rs9895420), and –211C>T (rs4793665), respectively (Table 2). Seven haplotypes were identified with a frequency ranging between 0.74 and 32.3% (Table 3). The linkage disequilibrium between each of the 3 SNPs, rs1989983, rs62059725, and rs9895420, was high (r^2 = 0.76 to 1.0) and rs62059725 and rs9895420 showed complete linkage. No deviations from the Hardy-Weinberg equilibrium were observed ($P > 0.05$).

Relationship between Genetic Variants and ABCC3 Expression Levels

No significant differences were observed in expression levels among samples with haplotype pattern 5, 6, or 7 (data not shown). None of the other SNPs were associated with changes in expression levels (data not shown).

Analysis of the DNA Methylation Status among Different Skin Samples by COBRA

DMD Fast Forward. Published on February 2, 2018 as DOI: 10.1124/dmd.117.079061
This article has not been copyedited and formatted. The final version may differ from this version.

After extensive examinations of 20 kbp up- and downstream of *ABCC3*, 9 CGIs were identified (Table 4). Among the 16 selected CG sites within CGIs, 3 (–308, –35, and +163 bp relative to TIS) were predominantly unmethylated, while another 3 (–16169, +9877, and +20266 bp relative to TIS) were heavily methylated. There was moderate to high methylation variability between skin samples, ranging between 4- and 153-fold in the remaining 10 CG sites (Figure 2A).

Relationship between ABCC3 mRNA Expression and DNA Methylation Levels

In order to analyze the relationship between ABCC3 expression and DNA methylation levels, we performed Spearman's regression analysis on real-time PCR and COBRA data from the 48 skin samples studied. As shown in Figure 2B, the DNA methylation levels of the CG site (–9718 loci relative to TIS) in CGI-6 negatively correlated with ABCC3 mRNA expression in skin samples. No other CGIs showed a negative correlation between ABCC3 mRNA expression and DNA methylation levels (data not shown).

Effects of CGI-6 on Transcriptional Activity of the ABCC3 promoter

In order to functionally evaluate CGI-6, we used different reporter gene constructs containing *ABCC3* promoter fragments and/or CGI-6 for reporter gene assays (Figure 3).

The results obtained indicated that CGI-6 exhibits no promoter activity. In contrast, luciferase activity was significantly higher in cells transfected with pGL4.10-CGI/Pro than in other cell cultures transfected with pGL4.10-Pro. These results indicate that CGI-6 exhibits regulatory activity and plays a role as an enhancer.

Increased ABCC3 Expression Induced by the 5-aza-dC Treatment

In order to evaluate the effects of DNA methylation on ABCC3 expression, we treated the HaCaT cell line with the DNA methyltransferase inhibitor, 5-aza-dC (Figure 4). The CGI-6 methylation status and ABCC3 mRNA expression levels were assessed by COBRA and real-time PCR. The treatment with 5-aza-dC led to a weaker methylation status in CGI-6 than in the control group (data not shown). A corresponding increase in ABCC3 mRNA was observed in cells exposed to the demethylating agent.

Decreased ABCC3 Expression Induced by CGI-6 Disruption Using the CRISPR/Cas9 System

In order to investigate the contribution of CGI-6 to ABCC3 mRNA expression, we disrupted the region surrounding CGI-6 in HaCaT cells using the CRISPR/Cas9 system. We confirmed targeted disruption by PCR amplification (Figure 5A, B) and direct

sequencing (data not shown). Quantitative real-time PCR showed significantly weaker ABCC3 mRNA expression in disrupted clones than in control clones (Figure 5C).

DMD Fast Forward. Published on February 2, 2018 as DOI: 10.1124/dmd.117.079061
This article has not been copyedited and formatted. The final version may differ from this version.

Discussion

An increasing number of studies recognize drug transporters as an important factor in pharmacokinetics as well as pharmacological and/or toxicological effects (Cascorbi 2006; Maeda and Sugiyama, 2008; Ieiri et al., 2009). Recent studies suggested that drug transporters play a role in the disposition of drugs in murine skin and human keratinocyte cell cultures (Schiffer et al., 2003; Heise et al., 2010; Hashimoto et al., 2013). These findings prompted speculation that inter-individual variability in the expression of drug transporters may lead to inappropriate drug levels and associated toxicity or inefficacy in skin. Thus, the identification of expressed drug transporters and their variability in human skin is important for elucidating the role of drug transporters in human skin. In the present study, we demonstrated large inter-individual differences in the expression of drug transporters in human skin. We also showed that DNA methylation in CGI located approximately 10 kbp upstream of *ABCC3* regulated its expression levels in normal human skin.

Twenty-two ABC and 15 SLC transporters were expressed at detectable levels in human skin, and ABCC3, SLCO3A1, SLC22A3, SLC16A7, ABCA2, ABCC1, and SLCO2B1 were strongly expressed in skin. In previous studies, expression comparisons among drug transporters in human skin tissues were limited to the findings of relative quantification

(Li et al., 2006; Takenaka et al., 2013; Fujiwara et al., 2014). We herein absolutely quantified, for the first time, the expression of drug transporters in human skin using a large number of skin tissues. It is important to note that the isoforms of expressed drug transporters in human skin were consistent with previous findings (Markó et al., 2012; Kielar et al., 2003; Li et al., 2006; Takenaka et al., 2013; Fujiwara et al., 2014). Previous studies showed constitutive expression of ABCC3 in NHEK by immunoblots and the functional ABCC-mediated efflux activity of NHEK using *in vitro* transport assay (Baron et al., 2001; Heise et al., 2010). Skin consists of heterogeneous cell populations such as keratinocytes and fibroblasts. Therefore, in order to evaluate the function of ABCC3, it is important to identify which cells and layers express ABCC3 in the future study.

Next, we focused on the mechanisms responsible for the variability in ABCC3 expression, which was the strongest in human skin, assuming that high mRNA levels are more relevant for transporter function. The variant analysis of the *ABCC3* gene showed that genetic polymorphisms in the promoter region of *ABCC3* did not correlate with the inter-individual variability in ABCC3 expression in human skin. This is not in agreement with previous studies showing that –211C>T significantly decreased ABCC3 mRNA levels in the human liver (Lang et al., 2004; Sasaki et al., 2011). One possible explanation for this discrepancy is transcription factors binding to the region including the –211T allele,

which is expressed in the human liver, but not in skin. On the other hand, our results are consistent with an *in vivo* analysis showing that –211C>T had no influence on ABCC3 expression levels in patients with acute leukemia (Doerfel et al., 2006). Further studies using human skin are required in order to clarify whether promoter variants contribute to ABCC3 expression in human skin. In addition to genetic polymorphisms, we analyzed the correlation between ABCC3 expression and age. Previous study suggested an age-associated decrease in the function of transporter (Toornvliet et al., 2006). In our study, the significant association was not observed (Supplemental Figure 1).

The epigenetic regulation of gene expression plays an important role in the inter-individual variability in the gene expression of drug transporters (Saito et al., 2011; Wu et al., 2015). We attempted to identify the underlying epigenetic mechanisms for inter-individual variability in ABCC3 mRNA expression in human skin. Our results showed that ABCC3 mRNA expression levels negatively correlated with the methylation levels of the CG site (–9718) in CGI-6 located approximately 10 kbp upstream of the *ABCC3* gene. Previous studies reported that DNA methylation in gene promoters plays an important role in gene transcription (Schaeffeler et al., 2011; Ikehata et al., 2012). However, our results revealed that methylation levels in CGIs surrounding the promoter of *ABCC3* did not affect ABCC3 mRNA expression. In order to investigate the role of

CGI-6 methylation in ABCC3 expression, we analyzed the methylation status of CGI-6 and ABCC3 mRNA levels in cells treated with or without a 5-aza-dC demethylating agent. The demethylation treatment of HaCaT cells led to about 2-fold reduction in the degree of methylation in CGI-6 (data not shown) and about 1.7-fold increase in ABCC3 mRNA levels. Previous studies reported that methylation of the *ABCC3* promoter region was not involved in ABCC3 mRNA levels in some cancer cell lines (Worm et.al, 2001; Zolk et al., 2013). These findings suggest that the methylation of CGI-6 plays a role in regulating ABCC3 mRNA expression in HaCaT cells.

CGIs are often located around or in more distant regions of gene promoters and their function is to regulate transcription (Deaton and Bird, 2011; Illingworth and Bird, 2009). The results of the luciferase reporter assay showed that CGI-6 did not exhibit promoter activity, but displayed activity, indicating an enhancer. Furthermore, in HaCaT cells, the disruption of the region surrounding CGI-6 led to significantly decreased ABCC3 mRNA levels. COBRA analysis revealed that CGI-6 was not hyper-methylated (about 50%) in HaCaT cells (data not shown), thus the disruption of CGI-6 caused reduced ABCC3 expression. These results suggest that CGI-6 regulates the transcriptional activity of *ABCC3*, and are consistent with previous findings showing that CGIs distant from the target gene locus affected gene expression (Yoon et al., 2005, 2009) while enhancers

located far from gene promoters regulated transcription (Ferreira et al., 2016; Hilton et al., 2015). Our results are also supported by previous findings showing that the methylation of enhancers affects gene expression (Yang et al., 2012; Hoivik et al., 2011). Few studies have examined the molecular mechanisms of transcriptional regulation of ABCC3. Luciferase assay with a series of truncated 5'-flanking regions indicated that the region from –127 to –23 bp is important for ABCC3 expression (Takada et al., 2000). In addition, it was demonstrated that ABCC3 is under the control of TATA-less promoter and Sp1 binding sites may be involved in the transcription. Another study reported that nuclear receptor retinoic X receptor-α-retinoic acid receptor-α (RXRα:RARα) function as a repressor of MRP3 activation by reducing Sp1 binding to –113 to –108 bp with respect to the *ABCC3* TIS (Chen et al., 2007). However, little studies have reported the relationship between ABCC3 expression and DNA methylation.

The CG site (–9718) showed the association with ABCC3 mRNA expression. The methylation levels in the CG site (–9718) was not positively associated with the other CG site (supplementary Figure 2). This result suggests that the CGI-6 including the CG site (–9718) play a key role in the inter-individual difference of ABCC3 expression in human skin. As a result of *in silico* search for transcriptional factors binding to CGI-6 (P-Match 1.0 Public, http://gene-regulation.com/pub/programs.html#pmatch), zinc finger protein

was predicted. It has been reported that a family of human zinc finger proteins bind to methylated DNA and repress transcription (Filion et al., 2006). Since a negative correlation was found between the DNA methylation status of CGI-6 and ABCC3 expression levels in human skin, the binding amount of zinc finger protein to CGI-6 may be changed depending on the DNA methylation status of CGI-6 and subsequently the transcription of ABCC3 may be regulated.

It was reported that inter-individual differences in ABCC3 protein expression in lung cancer strongly correlate with ABCC3 mRNA expression (Young et al., 1999 and 2001). Our study did not evaluate the protein expression in human skin. The importance of inter-individual differences in ABCC3 mRNA expression in human skin will be clarified by additional studies: correlation of mRNA levels with protein levels and drug transport in human skin.

In summary, we conducted a profile analysis of 26 ABC and 25 SLC transporter isoforms using a large number of skin tissues and showed that ABCC3 was expressed at the highest levels. The present study is the first to characterize the drug transporters expressed in human skin as absolute quantitative values. Our results showed that large inter-individual differences exist in the expression of drug transporters in human skin, and methylation levels in CGI contribute to the variability of ABCC3 expression in skin.

The role of transporters is not well known in human skin. ABCC1, which is one of the ABCC family, is expressed in keratinocytes. Interestingly, it was suggested that ABCC1 contributes to the transdermal absorption of substrate drug in human skin (Osman-Ponchet et al., 2014). Similar results were also reported in ABCB1 and ABCG2 (Hashimoto et al., 2013; Skazik et al., 2011). These reports suggest that ABC family in human skin has an important role in the transdermal absorption of their substrates, but the role of ABCC3 is not clear. The evaluation of the ABCC3 transport activities of the substrates is important to identify the contribution of the transdermal absorption in further study. To date, no clinically relevant drug-drug interactions involving ABCC3 have been reported. ABCC3 transports a wide range of substrates, such as endogenous substances (leukotriene C4, estradiol-17β-glucuronide), anticancer drugs (methotrexate, etoposide), and other drugs (acetaminophen glucuronide and fexofenadine) (Supplemental Table 7). Therefore, ABCC3 may be responsible for unexpected substance-induced reactions in skin. Our results will contribute to future studies on the disposition of endogenous and exogenous substances and may be very beneficial to the development of personalized medicine.

Acknowledgments

We appreciate the technical assistance provided by The Research Support Center, Research Center for Human Disease Modeling, Kyushu University Graduate School of Medical Sciences.

Authorship Contributions

Participated in research design: Takechi, Hirota, and Ieiri

Conducted experiments: Takechi, Hirota, Sakai, and Maeda

Performed data analyses: Takechi, Hirota, Sakai, and Maeda

Wrote or contributed to the writing of the manuscript: Takechi, Hirota, and Ieiri

References

Baron JM, Höller D, Schiffer R, Frankenberg S, Neis M, Merk HF, and Jugert FK (2001) Expression of multiple cytochrome p450 enzymes and multidrug resistance-associated transport proteins in human skin keratinocytes. *J Invest Dermatol* **116**:541–8.

Cascorbi I (2006) Role of pharmacogenetics of ATP-binding cassette transporters in the pharmacokinetics of drugs. *Pharmacol Ther* **112**:457-73.

Chen EC, Liang X, Yee SW, Geier EG, Stocker SL, Chen L, and Giacomini KM (2015) Targeted disruption of organic cation transporter 3 attenuates the pharmacologic response to metformin. *Mol Pharmacol* **88**:75-83.

Chen W, Cai SY, Xu S, Denson LA, Soroka CJ, Boyer JL (2007) Nuclear receptors RXRalpha:RARalpha are repressors for human MRP3 expression. *Am J Physiol Gastrointest Liver Physiol* **292**:G1221-7.

Deaton AM and Bird A (2011) CpG islands and the regulation of transcription. *Genes Dev* **25**:1010-22.

Doerfel C, Rump A, Sauerbrey A, Gruhn B, Zintl F, and Steinbach D (2006) In acute leukemia, the polymorphism -211C>T in the promoter region of the multidrug

resistance-associated protein 3 (MRP3) does not determine the expression level of the gene. *Pharmacogenet Genomics* **16**:149-50.

European Medicines Agency (2012) Guideline on the Investigation of Drug Interactions.

FDA Center for Drug Evaluation and Research (2012) Guidance for Industry : Drug Interaction Studies – Study Design, Data Analysis, Implications for Dosing, and Labeling Recommendations.

Ferreira LM, Meissner TB, Mikkelsen TS, Mallard W, O'Donnell CW, Tilburgs T, Gomes HA, Camahort R, Sherwood RI, Gifford DK, Rinn JL, Cowan CA, and Strominger JL (2016) A distant trophoblast-specific enhancer controls HLA-G expression at the maternal-fetal interface. *Proc Natl Acad Sci U S A* **113**:5364-9.

Filion GJ, Zhenilo S, Salozhin S, Yamada D, Prokhortchouk E, Defossez PA (2006) A family of human zinc finger proteins that bind methylated DNA and repress transcription. *Mol Cell Biol* **26**:169-81.

Fujiwara R, Takenaka S, Hashimoto M, Narawa T, and Itoh T (2014) Expression of human solute carrier family transporters in skin: possible contributor to drug-induced skin disorders. Sci Rep **4**:5251.

Gotanda K, Tokumoto T, Hirota T, Fukae M, and Ieiri I (2015) Sulfasalazine disposition in a subject with 376C>T (nonsense mutation) and 421C>A variants in the ABCG2 gene. *Br J Clin Pharmacol* **80**:1236-7.

Hashimoto N, Nakamichi N, Uwafuji S, Yoshida K, Sugiura T, Tsuji A, and Kato Y (2013) ATP binding cassette transporters in two distinct compartments of the skin contribute to transdermal absorption of a typical substrate. *J Control Release* **165**:54-61.

Heise R, Skazik C, Rodriguez F, Stanzel S, Marquardt Y, Joussen S, Wendel AF, Wosnitza M, Merk HF, and Baron JM (2010) Active transport of contact allergens and steroid hormones in epidermal keratinocytes is mediated by multidrug resistance related proteins. *J Invest Dermatol* **130**:305-8.

Hilton IB, D'Ippolito AM, Vockley CM, Thakore PI, Crawford GE, Reddy TE, and Gersbach CA (2015) Epigenome editing by a CRISPR-Cas9-based acetyltransferase activates genes from promoters and enhancers. *Nat Biotechnol* **33**:510-7.

Hoivik EA, Bjanesoy TE, Mai O, Okamoto S, Minokoshi Y, Shima Y, Morohashi K, Boehm U, and Bakke M (2011) DNA methylation of intronic enhancers directs

tissue-specific expression of steroidogenic factor 1/adrenal 4 binding protein (SF-1/Ad4BP). *Endocrinology* **152**:2100-12.

Huber RD, Gao B, Sidler Pfändler MA, Zhang-Fu W, Leuthold S, Hagenbuch B, Folkers G, Meier PJ, and Stieger B (2007) Characterization of two splice variants of human organic anion transporting polypeptide 3A1 isolated from human brain. *Am J Physiol Cell Physiol* **292**:C795-806.

Ieiri I, Higuchi S, and Sugiyama Y (2009) Genetic polymorphisms of uptake (OATP1B1, 1B3) and efflux (MRP2, BCRP) transporters: implications for inter-individual differences in the pharmacokinetics and pharmacodynamics of statins and other clinically relevant drugs. *Expert Opin Drug Metab Toxicol* **5**:703-29.

Ieiri I, Takane H, Hirota T, Otsubo K, and Higuchi S (2006) Genetic polymorphisms of drug transporters: pharmacokinetic and pharmacodynamic consequences in pharmacotherapy. *Expert Opin Drug Metab Toxicol* **2**:651-74.

Ikehata M, Ueda K, and Iwakawa S (2012) Different Involvement of DNA Methylation and Histone Deacetylation in the Expression of Solute-Carrier Transporters in 4 Colon Cancer Cell Lines. *Biol Pharm Bull* **35**:301–307.

Illingworth RS and Bird AP (2009) CpG islands – 'A rough guide'. *FEBS Lett* 583: 1713–1720.

International Transporter Consortium, Giacomini KM, Huang SM, Tweedie DJ, Benet LZ, Brouwer KL, Chu X, Dahlin A, Evers R, Fischer V, Hillgren KM, Hoffmaster KA, Ishikawa T, Keppler D, Kim RB, Lee CA, Niemi M, Polli JW, Sugiyama Y, Swaan PW, Ware JA, Wright SH, Yee SW, Zamek-Gliszczynski MJ, and Zhang L (2010) Membrane transporters in drug development. *Nat Rev Drug Discov* **9**:215-36.

Ita K (2016) Perspectives on Transdermal Electroporation. *Pharmaceutics* **8**:9.

Kielar D, Kaminski WE, Liebisch G, Piehler A, Wenzel JJ, Möhle C, Heimerl S, Langmann T, Friedrich SO, Böttcher A, Barlage S, Drobnik W, and Schmitz G (2003) Adenosine triphosphate binding cassette (ABC) transporters are expressed and regulated during terminal keratinocyte differentiation: a potential role for ABCA7 in epidermal lipid reorganization. *J Invest Dermatol* **121**:465-74.

Klatt S, Fromm MF, and König J (2011) Transporter-mediated drug-drug interactions with oral antidiabetic drugs. *Pharmaceutics* **3**:680-705.

Koepsell H (2015) Role of organic cation transporters in drug-drug interaction. *Expert Opin Drug Metab Toxicol* **11**:1619-33.

Kool M, van der Linden M, de Haas M, Scheffer GL, de Vree JM, Smith AJ, Jansen G, Peters GJ, Ponne N, Scheper RJ, Elferink RP, Baas F, and Borst P (1999) MRP3,

an organic anion transporter able to transport anti-cancer drugs. *Proc Natl Acad Sci U S A* **96**:6914-9.

Lane ME (2013) Skin penetration enhancers. *Int J Pharm* **447**:12-21.

Lang T, Hitzl M, Burk O, Mornhinweg E, Keil A, Kerb R, Klein K, Zanger UM, Eichelbaum M, and Fromm MF (2004) Genetic polymorphisms in the multidrug resistance-associated protein 3 (ABCC3, MRP3) gene and relationship to its mRNA and protein expression in human liver. *Pharmacogenetics* **14**:155-64.

Li Q, Tsuji H, Kato Y, Sai Y, Kubo Y, and Tsuji A (2006) Characterization of the transdermal transport of flurbiprofen and indomethacin. *J Control Release* **110**:542-56.

Ma Q and Lu AY (2011) Pharmacogenetics, pharmacogenomics, and individualized medicine. *Pharmacol Rev* **63**:437-59.

Maeda K and Sugiyama Y (2008) Impact of genetic polymorphisms of transporters on the pharmacokinetic, pharmacodynamic and toxicological properties of anionic drugs. *Drug Metab Pharmacokinet* **23**:223-35.

Markó L, Paragh G, Ugocsai P, Boettcher A, Vogt T, Schling P, Balogh A, Tarabin V, Orsó E, Wikonkál N, Mandl J, Remenyik E, and Schmitz G (2012) Keratinocyte

ATP binding cassette transporter expression is regulated by ultraviolet light. *J Photochem Photobiol B* **116**:79-88.

Neuvonen PJ, Niemi M, and Backman JT (2006) Drug interactions with lipid-lowering drugs: mechanisms and clinical relevance. *Clin Pharmacol Ther* **80**:565-81.

Osman-Ponchet H, Boulai A, Kouidhi M, Sevin K, Alriquet M, Gaborit A, Bertino B, Comby P, and Ruty B (2014) Characterization of ABC transporters in human skin. *Drug Metabol Drug Interact* **29**:91-100.

Prausnitz MR and Langer R (2008) Transdermal drug delivery. *Nat Biotechnol* **26**:1261-8.

Roth M, Obaidat A, and Hagenbuch B (2012) OATPs, OATs and OCTs: the organic anion and cation transporters of the SLCO and SLC22A gene superfamilies. *Br J Pharmacol* **165**:1260-87.

Saito J, Hirota T, Kikunaga N, Otsubo K, and Ieiri I (2011) Interindividual differences in placental expression of the SLC22A2 (OCT2) gene: relationship to epigenetic variations in the 5'-upstream regulatory region. *J Pharm Sci* **100**:3875-83.

Sasaki T, Hirota T, Ryokai Y, Kobayashi D, Kimura M, Irie S, Higuchi S, and Ieiri I (2011) Systematic screening of human ABCC3 polymorphisms and their effects on MRP3 expression and function. *Drug Metab Pharmacokinet* **26**:374-86.

Schaeffeler E, Hellerbrand C, Nies AT, Winter S, Kruck S, Hofmann U, van der Kuip H, Zanger UM, Koepsell H, and Schwab M (2011) DNA methylation is associated with downregulation of the organic cation transporter OCT1 (SLC22A1) in human hepatocellular carcinoma. *Genome Med* **3**:82.

Schiffer R, Neis M, Höller D, Rodríguez F, Geier A, Gartung C, Lammert F, Dreuw A, Zwadlo-Klarwasser G, Merk H, Jugert F, and Baron JM (2003) Active influx transport is mediated by members of the organic anion transporting polypeptide family in human epidermal keratinocytes. *J Invest Dermatol* **120**:285-91.

Schinkel AH and Jonker JW (2003) Mammalian drug efflux transporters of the ATP binding cassette (ABC) family: an overview. *Adv Drug Deliv Rev* **55**:3-29.

Schneck DW, Birmingham BK, Zalikowski JA, Mitchell PD, Wang Y, Martin PD, Lasseter KC, Brown CD, Windass AS, and Raza A (2004) The effect of gemfibrozil on the pharmacokinetics of rosuvastatin. *Clin Pharmacol Ther* **75**:455-63.

Shitara Y, Hirano M, Sato H, and Sugiyama Y (2004). Gemfibrozil and its glucuronide inhibit the organic anion transporting polypeptide 2 (OATP2/OATP1B1:SLC21A6)-mediated hepatic uptake and CYP2C8-mediated metabolism of cerivastatin: analysis of the mechanism of the clinically relevant

drug-drug interaction between cerivastatin and gemfibrozil. *J Pharmacol Exp Ther* **311**:228-36.

Skazik C, Wenzel J, Marquardt Y, Kim A, Merk HF, Bickers DR, Baron JM (2011) P-glycoprotein (ABCB1) expression in human skin is mainly restricted to dermal components. *Exp Dermatol 20*:450-2.

Takada T, Suzuki H, and Sugiyama Y (2000) Characterization of 5'-flanking region of human MRP3. *Biochem Biophys Res Commun* **270**:728-32.

Takai D and Jones PA (2003) The CpG island searcher: a new WWW resource. *In Silico Biol* **3**:235–240

Takenaka S, Itoh T, and Fujiwara R (2013) Expression pattern of human ATP-binding cassette transporters in skin. *Pharmacol Res Perspect* **1**:e00005.

Tamai I, Nezu J, Uchino H, Sai Y, Oku A, Shimane M, and Tsuji A (2000) Molecular identification and characterization of novel members of the human organic anion transporter (OATP) family. *Biochem Biophys Res Commun* **273**:251-60.

Toornvliet R, van Berckel BN, Luurtsema G, Lubberink M, Geldof AA, Bosch TM, Oerlemans R, Lammertsma AA, and Franssen EJ (2006) Effect of age on functional P-glycoprotein in the blood-brain barrier measured by use of (R)-

[(11)C]verapamil and positron emission tomography. *Clin Pharmacol Ther* **79**:540-8.

Worm J, Kirkin AF, Dzhandzhugazyan KN, and Guldberg P (2001) Methylation-dependent silencing of the reduced folate carrier gene in inherently methotrexate-resistant human breast cancer cells. *J Biol Chem* **276**:39990-40000.

Wu LX, Wen CJ, Li Y, Zhang X, Shao YY, Yang Z, and Zhou HH (2015) Interindividual epigenetic variation in ABCB1 promoter and its relationship with ABCB1 expression and function in healthy Chinese subjects. *Br J Clin Pharmacol* **80**:1109–1121.

Wu X, Kekuda R, Huang W, Fei YJ, Leibach FH, Chen J, Conway SJ, and Ganapathy V (1998) Identity of the organic cation transporter OCT3 as the extraneuronal monoamine transporter (uptake2) and evidence for the expression of the transporter in the brain. *J Biol Chem* **273**:32776-86.

Yang BT, Dayeh TA, Volkov PA, Kirkpatrick CL, Malmgren S, Jing X, Renström E, Wollheim CB, Nitert MD, and Ling C (2012) Increased DNA methylation and decreased expression of PDX-1 in pancreatic islets from patients with type 2 diabetes. *Mol Endocrinol* **26**:1203-12.

Yasar U, Greenblatt DJ, Guillemette C, and Court MH (2013) Evidence for regulation of UDP-glucuronosyltransferase (UGT) 1A1 protein expression and activity via DNA methylation in healthy human livers. *J Pharm Pharmacol* **65**:874–883.

Yoon B, Herman H, Hu B, Park YJ, Lindroth A, Bell A, West AG, Chang Y, Stablewski A, Piel JC, Loukinov DI, Lobanenkov V V, and Soloway PD (2005) Rasgrf1 Imprinting Is Regulated by a CTCF-Dependent Methylation-Sensitive Enhancer Blocker. *Mol Cell Biol* **25**:11184–11190.

Yoon BJ, Herman H, Sikora A, Smith LT, Plass C, and Soloway PD (2009) Regulation of DNA methylation of Rasgrf1. *Nat Genet* **30**:92–96.

Young LC, Campling BG, Voskoglou-Nomikos T, Cole SP, Deeley RG, and Gerlach JH (1999) Expression of multidrug resistance protein-related genes in lung cancer: correlation with drug response. *Clin Cancer Res* **5**:673-80.

Young LC, Campling BG, Cole SP, Deeley RG, and Gerlach JH (2001) Multidrug resistance proteins MRP3, MRP1, and MRP2 in lung cancer: correlation of protein levels with drug response and messenger RNA levels. *Clin Cancer Res* **7**:1798-804.

Zhou SF, Wang LL, Di YM, Xue CC, Duan W, Li CG, and Li Y (2008) Substrates and inhibitors of human multidrug resistance associated proteins and the implications in drug development. *Curr Med Chem* **15**:1981-2039.

Zolk O, Schnepf R, Muschler M, Fromm MF, Wendler O, Traxdorf M, Iro H, and Zenk J (2013) Transporter gene expression in human head and neck squamous cell carcinoma and associated epigenetic regulatory mechanisms. *Am J Pathol* **182**:234-43.

DMD Fast Forward. Published on February 2, 2018 as DOI: 10.1124/dmd.117.079061
This article has not been copyedited and formatted. The final version may differ from this version.

Footnotes

This work was supported by the Japan Research Foundation for Clinical Pharmacology.

DMD Fast Forward. Published on February 2, 2018 as DOI: 10.1124/dmd.117.079061
This article has not been copyedited and formatted. The final version may differ from this version.

Figure Legends

Figure 1. Quantification of ABC and SLC transporter mRNAs in Caucasian skin samples. (A) Absolute transporter mRNA levels were evaluated in human skin samples (n=18). Regarding absolute quantification, each 96-well assay plate contained unknown samples and sequentially diluted concentrations of the plasmid standard constructed, from which a standard curve was generated for the quantification of gene copy numbers in unknown samples. In order to compare gene expression levels among different samples, the amount of target mRNA was corrected to that of GAPDH. (B) The mean mRNA expression level of each transporter is expressed as a percentage of the total mean transporter mRNA content.

Figure 2. Correlation analysis between ABCC3 mRNA levels and methylation frequencies of CGI in Caucasian skin samples. (A) DNA methylation differences in CGIs surrounding the *ABCC3* gene. Relative methylation frequencies were assessed by COBRA using human skin samples (n=48). The y-axis represents the band intensity ratio of the methylated status to unmethylated status. The x-axis represents the CG locus relative to TIS. (B) Negative correlation between ABCC3 mRNA expression and

DMD Fast Forward. Published on February 2, 2018 as DOI: 10.1124/dmd.117.079061
This article has not been copyedited and formatted. The final version may differ from this version.

methylation levels at the CG site (–9718 loci relative to TIS) in CGI-6 (n=48). *Rs* and *P* value are from Spearman's rank-order correlation analysis.

Figure 3. Effects of CGI-6 on luciferase activities. Luciferase (Luci) reporter gene constructs were transiently transfected into HaCaT cells. Luciferase values are normalized to the pRL-TK vector. Data represent the mean ± SD (n=4) and mean value obtained with the pGL4.10-basic vector as 100%. * $P < 0.05$: statistically analyzed using the Student's *t*-test.

Figure 4. Effects of 5-aza-dC on ABCC3 mRNA expression in HaCaT cells. HaCaT cells were treated with 3 μmol/L 5-aza-dC for 72 hr. ABCC3 mRNA expression levels were assessed using real- time PCR and normalized to the expression of GAPDH. Data represent the mean ± SD of triplicate experiments. * $P < 0.05$: statistically analyzed using the Student's *t*-test.

Figure 5. Effects of the deletion of CGI-6 on ABCC3 mRNA expression in HaCaT cells. (A) Electrophoresis of PCR products spanning the deleted region locus. (B) Quantification of CGI-6 by real-time PCR using primers located on the inside of the

deleted region. Data represent the mean±SD and results were normalized to the region of the *ACTB* gene. (C) Each ABCC3 mRNA level in the established clones was assessed by real-time PCR. Data represent the mean ± SD (four control clones and three deleted clones) and results were normalized to GAPDH mRNA levels. **P* < 0.05: statistically analyzed using the Student's *t*-test.

DMD Fast Forward. Published on February 2, 2018 as DOI: 10.1124/dmd.117.079061
This article has not been copyedited and formatted. The final version may differ from this version.

TABLE 1

First step screening for the evaluation of transporter expression in Caucasian skin samples

Gene	C_t Mean	Gene	C_t Mean	Gene	C_t Mean	Gene	C_t Mean
ABCA1	28.9	*ABCC2*	33.4	*SLC15A1*	30.6	*SLC22A8*	>35
ABCA2	29.1	*ABCC3*	27.0	*SLC15A2*	32.5	*SLC22A10*	>35
ABCA3	31.1	*ABCC4*	32.2	*SLC16A1*	29.7	*SLC22A11*	>35
ABCA4	>35	*ABCC5*	28.4	*SLC16A3*	33.3	*SLC46A1*	32.5
ABCA5	29.0	*ABCC6*	32.2	*SLC16A7*	30.0	*SLC47A1*	29.2
ABCA6	32.3	*ABCC8*	>35	*SLC16A8*	>35	*SLC47A2*	30.4
ABCA7	30.7	*ABCC10*	33.2	*SLC22A1*	32.9	*SLCO1A2*	>35
ABCA8	31.2	*ABCC11*	33.6	*SLC22A2*	>35	*SLCO1B1*	>35
ABCA9	32.1	*ABCC12*	>35	*SLC22A3*	28.6	*SLCO1B3*	>35
ABCA10	31.2	*ABCG1*	29.9	*SLC22A4*	33.0	*SLCO2B1*	30.1
ABCA12	31.8	*ABCG2*	32.9	*SLC22A5*	30.2	*SLCO3A1*	28.9
ABCB1	32.1	*ABCG5*	34.4	*SLC22A6*	>35	*SLCO4A1*	33.7
ABCC1	29.3	*ABCG8*	>35	*SLC22A7*	>35		

In easy comparisons (first screening), the mean cycle threshold (C_t) value of each transporter was calculated. One-sixteenth of pooled cDNA was used as a template for real-time PCR. Pooled cDNA was prepared by mixing an identical volume of cDNA (n=20). C_t values of > 35, in the range of 31 to 35, and < 31 were interpreted as the absence of gene expression, the presence of gene expression, but below the limit of quantitation, and the presence of gene expression at the quantitative level, respectively.

TABLE 2

***ABCC3* genetic variations in Caucasian skin samples**

Position[a)]	Reference allele[b)]	Variant allele	Genotype			Frequency of variant allele (%)	HW *P* val	NCBI SNP ID
			R / R	R / V	V / V			
–1767	agagGcatc	agagAcatc	39	9	0	9.4	1.0000	rs1989983
–1328	gcttGcccc	gcttAcccc	46	2	0	2.1	1.0000	rs72837520
–1213	tggaCagac	tggaGagac	41	7	0	7.3	1.0000	rs62059725
–897	ccttCcccc	cctt–cccc	24	17	7	32.3	0.2858	rs35467079
–260	tggcTtggc	tggcAtggc	41	7	0	7.3	1.0000	rs9895420
–211	ccccCacct	ccccTacct	10	18	20	60.4	0.2026	rs4793665

a), With respect to the TIS of the *ABCC3* gene; A in ATG is designated as +1 and that immediately following the 5' base is designated as –1.; b), GenBank accession no. NC_000017.11; R, reference allele; V, variant allele; HW *P* val, Hardy-Weinberg *P* value

TABLE 3

Estimated haplotypes in *ABCC3* gene in Caucasian skin samples

Haplotype	–1767G>A	–1328G>A	–1213C>G	–897delC	–260T>A	–211C>T	Frequency (%)
#1	A	A	G	C	A	C	0.74
#2	A	G	C	C	T	C	2.08
#3	A	G	G	C	A	C	6.56
#4	G	A	C	C	T	C	1.35
#5	G	G	C	C	T	C	28.9
#6	G	G	C	C	T	T	28.1
#7	G	G	C	Del	T	T	32.3

Nucleotides that are different from the reference sequence are underlined. Del represents the deletion of the nucleotide.

DMD Fast Forward. Published on February 2, 2018 as DOI: 10.1124/dmd.117.079061
This article has not been copyedited and formatted. The final version may differ from this version.

TABLE 4

Location of CGIs in the region surrounding *ABCC3*

Name	Start[a)]	End[a)]	%GC	Obs/Exp	Length (bp)
CGI-1	–20090	–19881	53.3	0.603	210
CGI-2	–16357	–16153	56.6	0.600	205
CGI-3	–15643	–15423	50.7	0.608	221
CGI-4	–13873	–13600	60.6	0.604	274
CGI-5	–13448	–13221	57.5	0.603	228
CGI-6	–9874	–9674	57.7	0.600	201
CGI-7	–429	502	70.7	0.732	931
CGI-8	9717	10205	54.4	0.611	489
CGI-9	19852	20429	53.6	0.657	578

a) With respect to the TIS of the *ABCC3* gene.

DMD Fast Forward. Published on February 2, 2018 as DOI: 10.1124/dmd.117.079061
This article has not been copyedited and formatted. The final version may differ from this version.

Figure 1

A

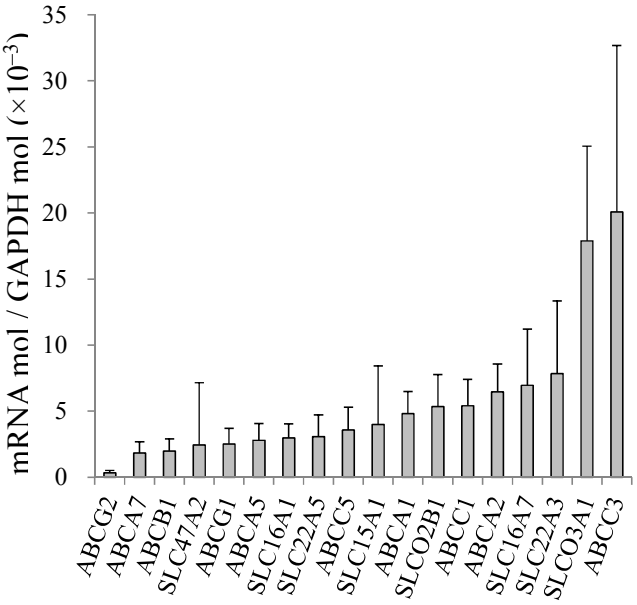

B

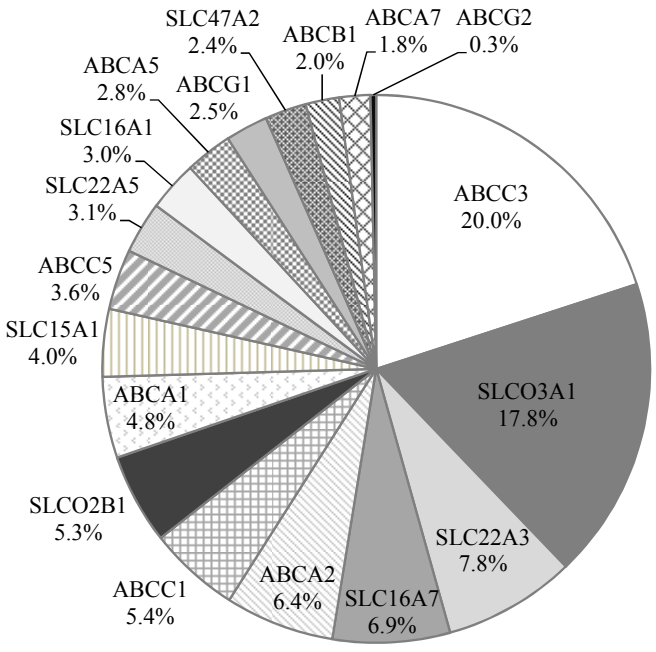

DMD Fast Forward. Published on February 2, 2018 as DOI: 10.1124/dmd.117.079061
This article has not been copyedited and formatted. The final version may differ from this version.

Figure 2

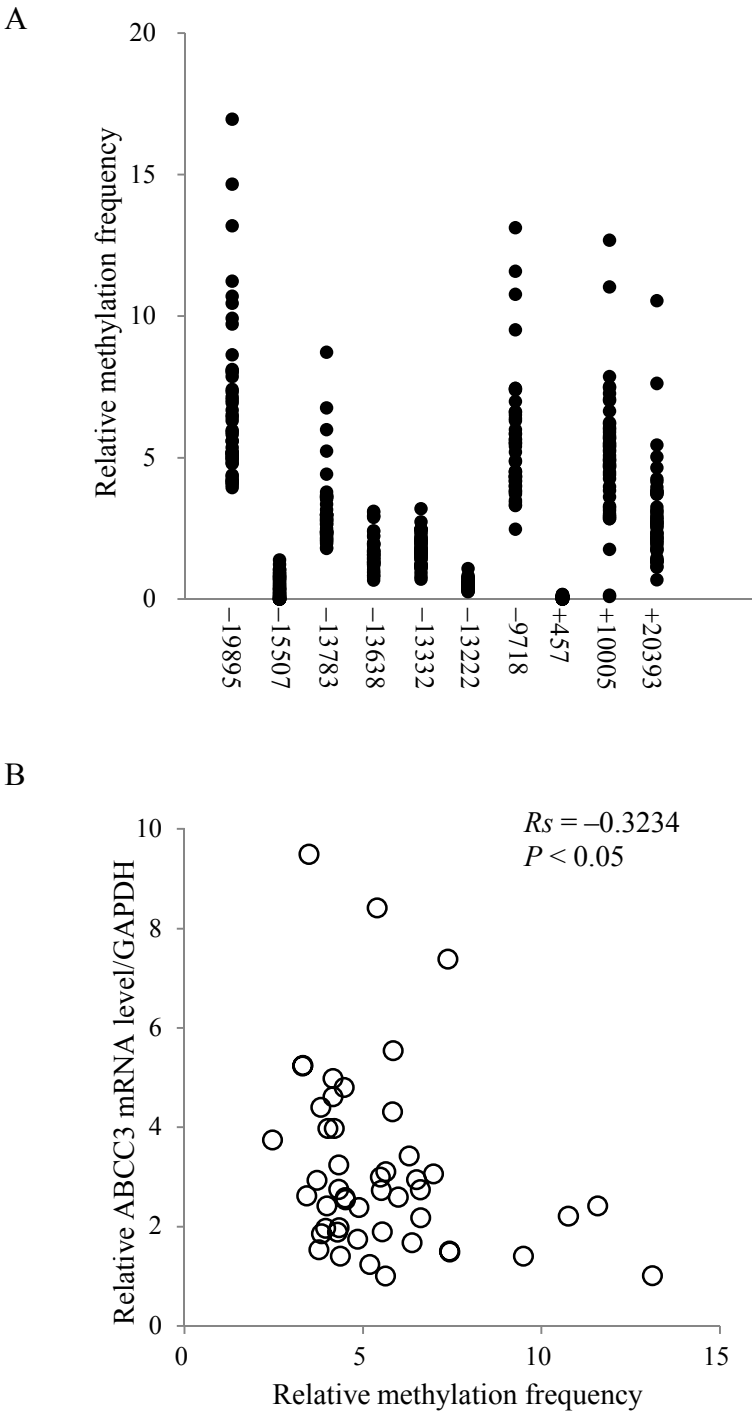

DMD Fast Forward. Published on February 2, 2018 as DOI: 10.1124/dmd.117.079061
This article has not been copyedited and formatted. The final version may differ from this version.

Figure 3

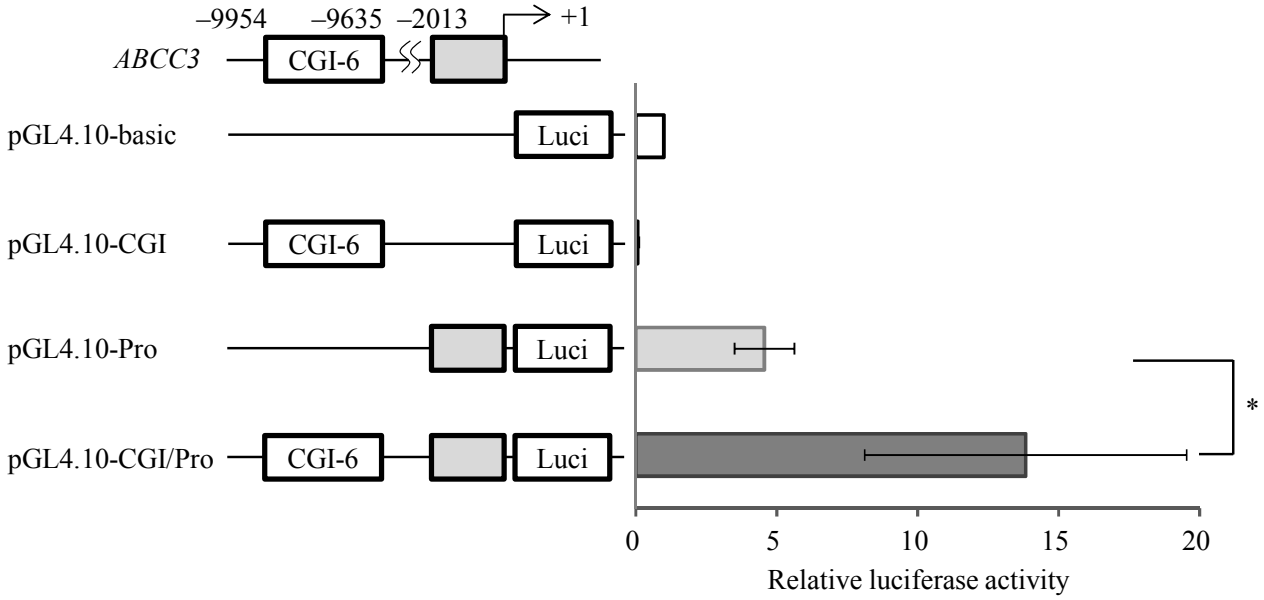

DMD Fast Forward. Published on February 2, 2018 as DOI: 10.1124/dmd.117.079061
This article has not been copyedited and formatted. The final version may differ from this version.

Figure 4

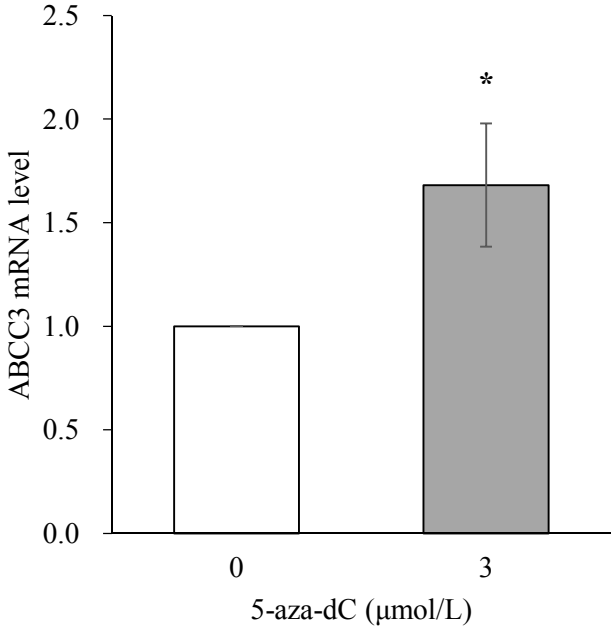

DMD Fast Forward. Published on February 2, 2018 as DOI: 10.1124/dmd.117.079061
This article has not been copyedited and formatted. The final version may differ from this version.

Figure 5